

Hydrogeochemical Evolution and Appraisal of Groundwater Quality in Panna District, Central India

Pankaj Kumar¹ · Alok Kumar^{2,3} · Chander Kumar Singh² · Chitresh Saraswat¹ · Ram Avtar¹ · A. L. Ramanathan² · Srikantha Herath¹

Received: 27 June 2015 / Revised: 19 September 2015 / Accepted: 20 September 2015 / Published online: 19 November 2015
© Springer Science+Business Media Dordrecht 2015

Abstract Intense agricultural and mining/industrial activities make groundwater quality vulnerable to contaminants. This study conducted in one of the mining areas of Panna district evaluated the factors influencing the groundwater hydrogeochemistry using water quality parameters and multi-isotopic approach considering the fact that groundwater is the only major source of drinking water. Forty-five water samples comprising both shallow and deep aquifers were collected and analyzed for major ions, $\delta^{18}\text{O}$, and δD . The geochemical data were used to characterize and classify water samples based on a multitude of ion plots and diagrams. The groundwater in the region is found to be contaminated with fluoride and nitrate. The sources for fluoride are mostly geogenic in nature. The alkaline nature of groundwater triggers replacement of the exchangeable fluoride from minerals like biotite/muscovite and results in its enrichment. In addition, it is contributed through leaching of fluorides from granitic rocks, abundantly present in the study area. The weathering of these fluoride-bearing minerals releases fluoride into the groundwater. On the other hand, nitrate enrichment is mainly attributed to leaching from untreated sewerage system and agricultural runoff containing nutrients from excess use of fertilizers. The stable isotopic

composition for most of the collected samples was found to be near the local meteoric water line (LMWL), i.e., origin of ground water is meteoric in principle; however, the point away from the LMWL might favor exchange with rock minerals and evaporation processes. This study sets an important background for decision makers to take the suitable countermeasures from the public health perspective for sustainable water resources management.

Keywords Hydrogeochemistry · Isotopes · Nitrate · Fluoride · Panna

Introduction

Groundwater is finite but replenishable as a resource. The quality and quantity of this resource is critical for food supplies, public health and transportation, etc. and has a profound impact on society with respect to quality of life (Gupta and Deshpande 2004). Madhya Pradesh lying in the peninsular Deccan trap region has poor to moderate groundwater potential. Groundwater in such formations occurs in the weathered and fractured zones. The limited availability of groundwater and scarcity of sustainable water supply has resulted in over-exploited blocks and stress on groundwater regime. The groundwater demand has been increasing abruptly over past few decades due to its growing usage for drinking, irrigation, and industrialization along with deterioration of surface water resources (Reddy 2012). The change in ionic assemblage of different aquifer system is due to cumulative effect of indigenous geological signature, dominant anthropogenic activities, and land use/land cover (LU/LC) pattern (Basnyat et al. 1999; Osborne and Wiley 1988; Roth et al. 1996; Subramani et al. 2005). The groundwater quality is controlled by

✉ Pankaj Kumar
pankajenvsci@gmail.com

¹ Institute for the Advanced Study of Sustainability (UNU-IAS), United Nations University, 5-53-70, Shibuya-ku, Tokyo 150-8925, Japan

² School of Environmental Sciences, Jawaharlal Nehru University, New Delhi, India

³ Department of Environmental Science, Central University of Rajasthan, Kishangarh, Ajmer, Rajasthan, India

several factors, including climate, soil characteristics, manner of circulation of groundwater through the rock types, area topography, etc. (Reghunath et al. 2002; Singh et al. 2004). Generally, aquifers in irrigated agricultural regions become salinized by a variety of mechanisms, including naturally occurring salts in the parent aquifer material, surface water importation, lateral flows from an adjacent saline aquifer, salt water intrusion, and lack of sufficient drainage. Apart from these factors, the interaction between the groundwater and river water and the mixing and non-mixing of different types of groundwater may also play important roles in determining the groundwater quality (Reghunath et al. 2002). Intense agricultural practices have led to the incessant use of fertilizers and groundwater abstraction resulting in water quality degradation.

Henceforth, water quality monitoring has been given the highest preference in health protection (World Health Organization 2006). With attaining the physico-chemical signature of ground water, hydro-geochemist unearth the possibilities of suitability of water for different purposes and study its chemical evolution processes. In other words, assessment of groundwater quality is needed to ensure its usability in different sectors in a safe manner (Vijith and Satheesh 2007).

While more than seventeen percent of the world population resides in India, they have access to only four percent of the world's freshwater resources (Singh 2003). Despite this water scarcity, groundwater is being extracted non-judicially without due consideration to quality issues (Ravindra and Garg 2007). Various studies reported issues related to groundwater quality (contamination with lethal chemicals like arsenic, nitrate, fluoride, and heavy metals) and quantity (water budget deficit) in different parts of India (CGWB 2010).

The Panna district in central India is famous for its diamond supply and has witnessed intense agricultural and mining/industrial activities in the last few decades which is likely to make groundwater vulnerable with respect to its quality. Despite its importance, very limited number of authentic information about water quality in this area leaves an enormous gap for policy makers as well as local consumers to give a fruitful thought about water resource management. So, the objective of this study was to understand the origin, processes, and the mechanisms for the geochemical evolution of groundwater as well as to highlight the causes of groundwater quality deterioration in Panna district of Madhya Pradesh. The results would constitute an important background for decision makers to take the suitable countermeasures for sustainable water resources management.

Study Area

Panna district of Bundelkhand, Madhya Pradesh, is located between 23°45' and 25°10' N latitudes and 79°45' and 80°40' E longitude and has a common border with Banda district of Uttar Pradesh and Chhatarpur, Damoh, Jabalpur, and Satna districts of Madhya Pradesh (Fig. 1). It has a total geographical area of 7135 km². The climate of the area is warm, sub-humid, sub-tropical, and monsoon type. May is the hottest month, while January is the coldest month throughout the year. The mean maximum and minimum temperatures are 27.9, 45.2, and 15.9 °C respectively. The average annual rainfall is 112 cm. About 93.5 % of the total rainfall is received during June to September by the southwest monsoon. Maximum rainfall is received during the month of July and August. Ken River and its tributaries are main drainages of Panna (Singh et al. 1983). The altitude/elevation of the area ranges from 150 to 450 m above MSL.

The topography of Panna is mostly hilly and traversed by hills and valleys. The greater part of its area lies on the branch of Vindhyan, known as Panna range, which traverses Bundelkhand from the southwest to the northeast. Geological map of the study area is shown in Fig. 2. The southern Panna district forms a plateau which was formed by cascade type rocks of Vindhyan series. Geologically, northern part of the area belongs to the Archaeans and Vindhyan systems. Archaeans are composed of old metamorphics, granites, gneisses, and schists. They are hard and compact formations with low primary permeability forming poor aquifers. Vindhyan are composed of sandstone, shale, and limestone. The sandstone and shale are hard and compact and form poor aquifers. Ground water occurs only in these weathered mantle and underlying fractured zone below. The limestone is different in its hydrogeological properties having large solution cavities that give rise to immense secondary permeability. In the study area, alluvium comprises unconsolidated gravel, sand, silt, and clay in various proportions and has primary intergranular porosity and permeability. Mineralogically, this area is being dominated by granitic rocks with pegmatites, amphibolites, quartz and feldspar, and large deposits of marine bluish/mottled clays, and conglomeratic gravels (Krishnan 1960). The Panna range consists principally of the Rewa sandstone of the Vindhyan rocks and has long been famous for its diamond mines. The diamonds occur as pebbles in a conglomerate, and also in pebbly clay derived from it by disintegration. The Bundelkhand granite rocks are found in Ajaigarh Tehsil of Panna district (Avtar et al. 2013).

Fig. 1 Study area map with sampling locations

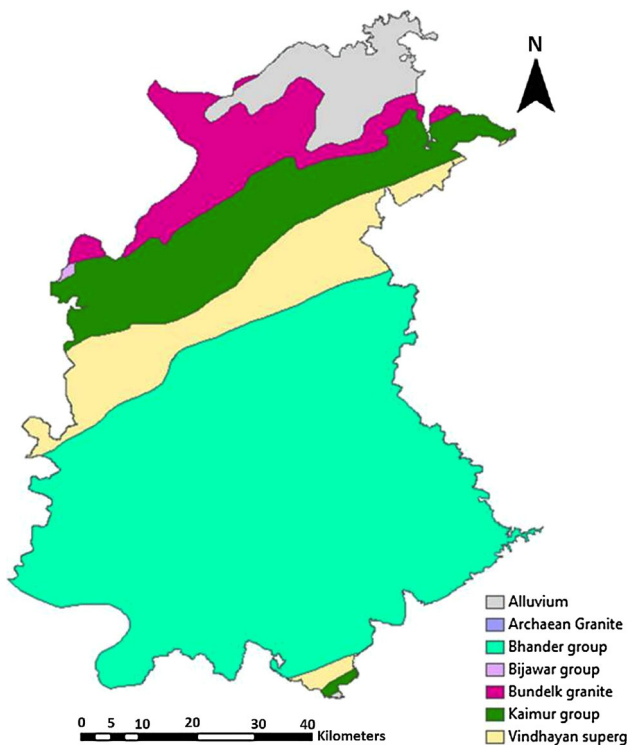
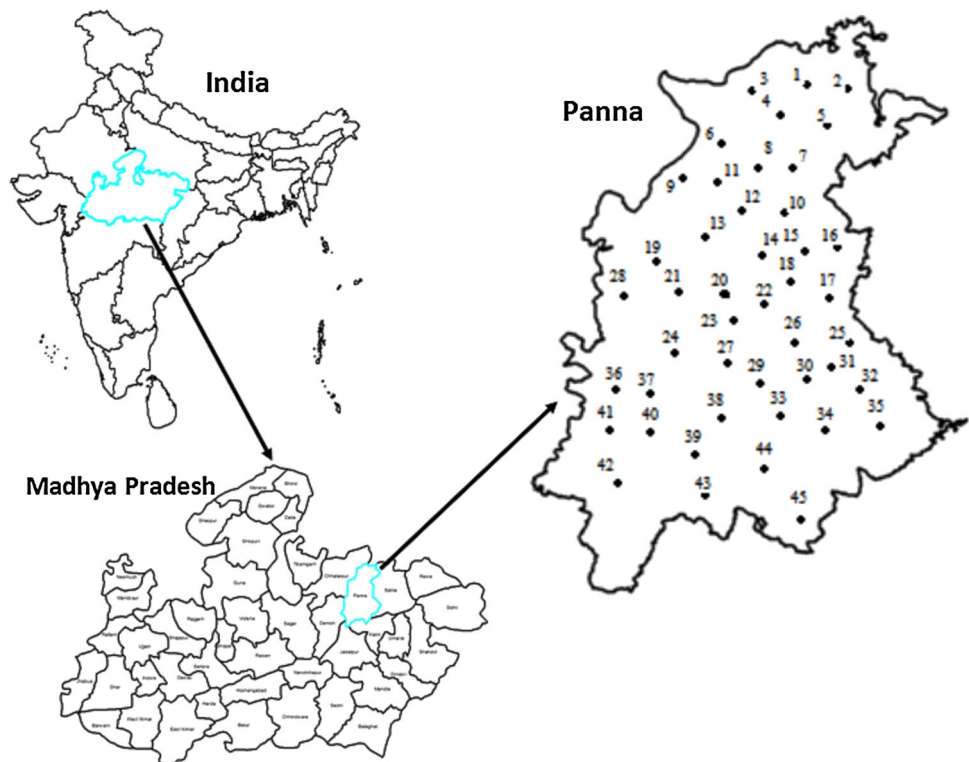


Fig. 2 Geological map of the study area

The land use/land cover (LULC) map was generated using the unsupervised classification of Landsat TM data for the year 2005. LULC analysis is useful to assess

probable impacts of change in the LULC on the land and water resources. The area was classified into ten categories, viz. Water body, dense forest, waterlogged, built-up, current fallow, degraded forest, land with scrub, barely exposed rock, fallow land, and land without scrub (Fig. 3). Percentage distribution of different classes is also shown in Table 1. Dense forest dominates the area because of the presence of the Panna Tiger Reserve. This is followed by current fallow and agricultural land.

Sampling and Analytical Techniques

The study area was divided into several grids from where representative groundwater samples were collected. The area of the grid was about $12 \times 12 \text{ km}^2$, and 45 samples were collected on the basis of spectral signature observed on satellite image from different grids during the month of May 2010 (Fig. 1). The conditions of vegetation show the subsurface manifestation of the groundwater. Most of the groundwater samples were collected from open wells, dug wells, bore wells, and hand pumps at various depths ranging from 5 to 30 m below ground level. The sample coordinates were recorded using Global Positioning System (GPS III, Garmin).

On-site measurements of the electrical conductivity (EC), pH, and temperature were made using an in-line flow cell to ensure the exclusion of atmospheric contamination

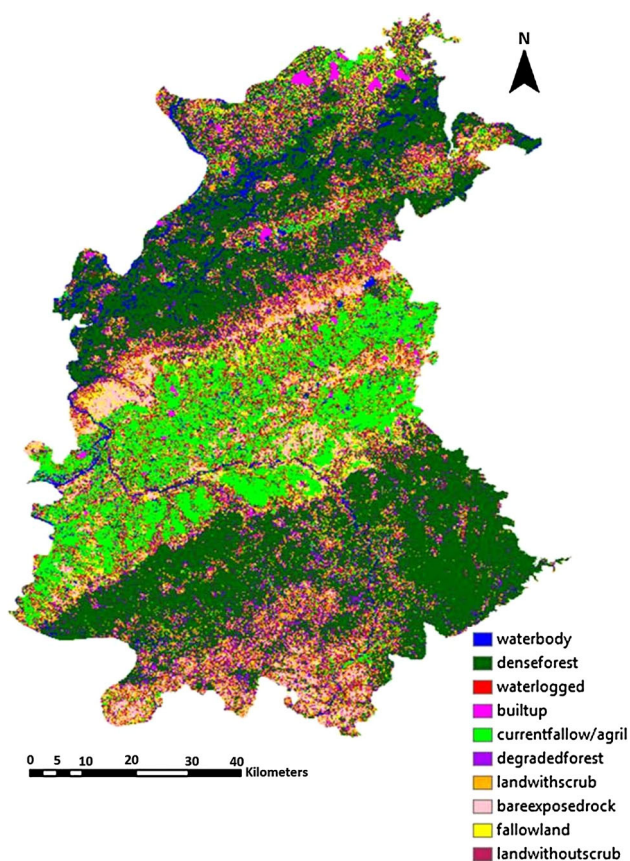


Fig. 3 Land use–land cover map of the study area

Table 1 Land use/land cover classes and their percentage in the study area

Sr No.	Class name	Area (Km ²)	Percentage
1	Water body	177.0	2.6
2	Dense forest	2689.9	40.1
3	Water logged	168.9	2.5
4	Built-up	46.3	0.7
5	Current fallow/agriculture area	1031.7	15.4
6	Degraded forest	673.7	10.0
7	Land with scrub	706.5	10.5
8	Bare exposed rock	298.8	4.4
9	Fallow land	250.3	3.7
10	Land without scrub	673.3	10.0

and to minimize the fluctuations. The portable Orion Thermo water analyzing kit (Model Beverly, MA, 01915) with a precision of 1 % was used for all on-site measurements. Three samples were collected from each location and filtered using 0.2- μm Millipore membrane filters. The samples collected for major ions analysis were acidified using 1 % HNO_3 to stabilize trace metals ($\text{pH} \sim 2$), while samples collected for nitrate were acidified with H_3BO_3

(Kumar et al. 2010). Samples were brought to the laboratory in an ice chest and stored below 4 °C. The samples were analyzed for the anion, cations, and trace metals like Fe, Mn, and Zn. The concentration of HCO_3^- was analyzed by acid titration (using Metrohm Multi-Dosimat), while other anions Cl^- , NO_3^- , SO_4^{2-} , F^- , and PO_4^{3-} were analyzed by DIONEX ICS-90 ion chromatograph with an error percentage of <2 % using duplicates. Major cations and trace elements were determined with inductively coupled plasma-mass spectrometry (ICP-MS) with a precision of <1 % using duplicates. Oxygen and hydrogen isotopes were analyzed by the mass spectrometer (MODEL MAT 252, Thermo Finnigan Inc.) at the University of Tsukuba. The results for both isotopes were expressed through deviation from the VSMOW (Vienna Standard Mean Ocean Water) standard using the δ -scale according to Eq. (1) and the unit is per mil.

$$\delta\% = \left[\frac{R_{\text{Sample}} - R_{\text{VSMOW}}}{R_{\text{VSMOW}}} \right] \times 1000, \quad (1)$$

where R is the isotopic ratio (i.e., $^2\text{H}/^1\text{H}$ and $^{18}\text{O}/^{16}\text{O}$) for the sample and standard. For the sample preparation before isotopic measurement, we adopted hydrogen gas equilibrium method using a platinum catalyst with 6 h for δD and carbon dioxide gas equilibrium method with 9 h for $\delta^{18}\text{O}$. Analytical precisions of stable isotopes were better than 0.1 ‰ for $\delta^{18}\text{O}$, 1.0 ‰ for δD , and ± 0.000007 for $^{87}\text{Sr}/^{86}\text{Sr}$. For major ions, analytical precision was checked by normalized inorganic charge balance (NICB) (Agrawal et al. 2011). This is defined as $[(T_z^+ - T_z^-)/(T_z^+ + T_z^-)]$ and represents the fractional difference between total cations and anions. The observed charge balance supports the quality of the data points, which is better than ± 5 %, and generally, this charge imbalance came in favor of the positive charge.

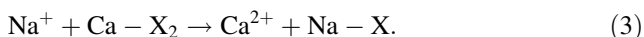
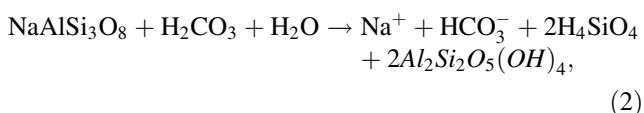
Results and Discussion

Major Ion Chemistry

Physicochemical Parameters

The statistical summary of physicochemical parameters analyzed is presented in Table 1. The pH value of groundwater is ranging between 7.16 and 8.02 reflecting the weak alkaline condition of groundwater. Low variation of pH with low value of standard deviation (SD) being 0.20 among the different samples indicates that groundwater studied here may be attributed to the aquifers with single type of formation (Reddy 2012). The electrical conductivity (EC) of the water samples ranges from 140.5 to 1092 $\mu\text{S}/\text{cm}$ with an average value of 411.38 $\mu\text{S}/\text{cm}$. High EC values

indicate increased concentration of dissolved solids and/or high ionic strength of the groundwater, local variation in soil type, and agricultural activities in the area. It is found that Na^+ , Ca^{2+} , and Mg^{2+} together contributed 96.81 % of total cations, whereas Cl^- , HCO_3^- , and SO_4^{2-} contributed about 91.0 % of total anions in the study area. Among anions, the average abundance trend found was in the order $\text{HCO}_3^- > \text{Cl}^- > \text{NO}_3^- > \text{SO}_4^{2-} > \text{PO}_4^{3-} > \text{F}^-$. On the other hand, the dominant cation was Na^+ followed by Ca^{2+} , NH_4^+ , Mg^{2+} , and K^+ . Processes like weathering of rocks or minerals containing Na (like quartzite, schist, and granitic rocks which are in abundance in the study area) and cation exchange (interchange of Na^+ and K^+ by Ca^{2+} and Mg^{2+} sorbed on the surface of clay) are mainly responsible for the dominance of Na^+ and Ca^{2+} in the groundwater samples (Srinivasamoorthy et al. 2008). Mechanisms for both processes of feldspar weathering and cation exchange are shown in Eqs. 2 and 3, respectively:



Here, for Eq. 3, Na^+ is adsorbed by the exchanger X, while Ca^{2+} is released and Ca- HCO_3 -type water results.

The relation between T_z^+ (here T_z^+ defined as the sum of all major cations, i.e., Ca^{2+} , Mg^{2+} , Na^+ , and K^+) versus (Ca^{2+} and Mg^{2+}) and (Na^+ and K^+) is shown by the (1:1) scatter plot (Fig. 4). Significant linear association was found between (Na^+ and K^+) and T_z^+ (with $R^2 = 0.81$ and calculated p value = 0.000027) in contrast to the poor trend found between (Ca^{2+} and Mg^{2+}) and T_z^+ (with $R^2 = 0.16$ and calculated p value = 0.108). This result supports the idea for dominance of carbonate weathering of silicate minerals that enrich the water samples both in terms of Na^+ and HCO_3^- , which is explained by Eqs. 4 and 5:

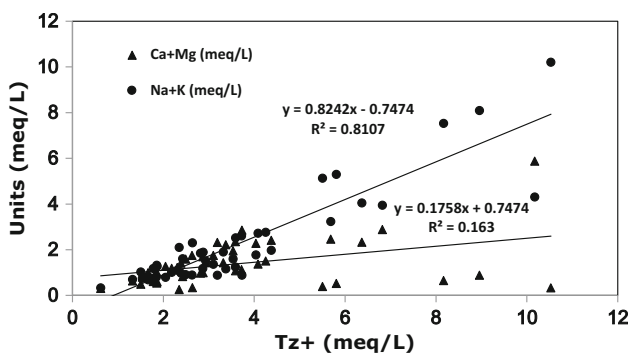
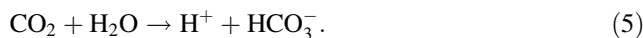
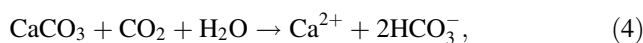
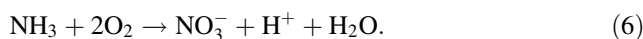


Fig. 4 Scatter plot showing the relation between T_z^+ versus (Ca^{2+} and Mg^{2+}) and (Na^+ and K^+). Here T_z^+ is defined as the sum of all major cations, i.e., Ca^{2+} , Mg^{2+} , Na^+ , and K^+



Most dominant anion HCO_3^- varied in range of 142.48–486.27 mg/L. This high concentration of HCO_3^- is an indicator of carbonate weathering and decomposition of organic matter (Avtar et al. 2013). Except for few, Cl^- concentration in most of the water samples lies within the recommended maximum permissible as well as desirable limits from WHO. i.e., 600 and 200 mg/L, respectively. The relatively higher concentration of Cl^- in some samples can be attributed to anthropogenic activities, e.g., the input from sewage effluents and high rate of evaporation during recharge at spatial scale. The concentration of SO_4^{2-} in groundwater samples was found to range from 1.23 to 140.69 mg/L. The study region has intense agriculture activity, and thus, the enrichment of groundwater from SO_4^{2-} can be supported by the fact that the breakdown of organic matter and agriculture runoff may be contributing to unutilized SO_4^{2-} (Anderson 1979).

NO_3^- and F^- concentrations are of major concern from the viewpoint of human health as 34 and 30 % of the water samples are found to be higher than the permissible limit as prescribed by WHO. The concentration of NO_3^- varied from 0.04 to 118.55 mg/L with an average value of 22.43 mg/L. High concentration of NO_3^- in groundwater (especially samples number 25, 26, 29, 30, 31, 36, 37, 40, and 41) clearly indicated an excessive use of fertilizers in agricultural areas, which is evident from the LULC of study region (Fig. 3), as well as microbial mineralization in the groundwater (Kumar et al. 2011). To support this idea, groundwater level map for this area is shown in Fig. 5. Here it is found that area dominated by agricultural activity has severe drawdown of groundwater resulting into lowering the ground water level. Nitrate pollution in mainly concentrated in the area represented by lower groundwater level. The process of nitrification responsible for conversion of ammonia within nitrogen fertilizers into nitrate is shown in Eq. (6):



To make a deep insight into the influence of different possible anthropogenic activities for nitrate enrichment in the water samples, different plots are shown in Fig. 6. The NO_3^- – K^+ plot (Fig. 6a) suggests significant contribution from agricultural runoffs; however, the points lying near to NO_3^- axis (indicated by dotted line circle) show input of nitrate from other possible sources like leaching from untreated sewerage system. The NO_3^- – Cl^- plot (Fig. 6b) shows significant association that indicates common origin of both the ions, i.e., domestic sewerage as rural setting is identified to increase both NO_3^- and Cl^- contents in

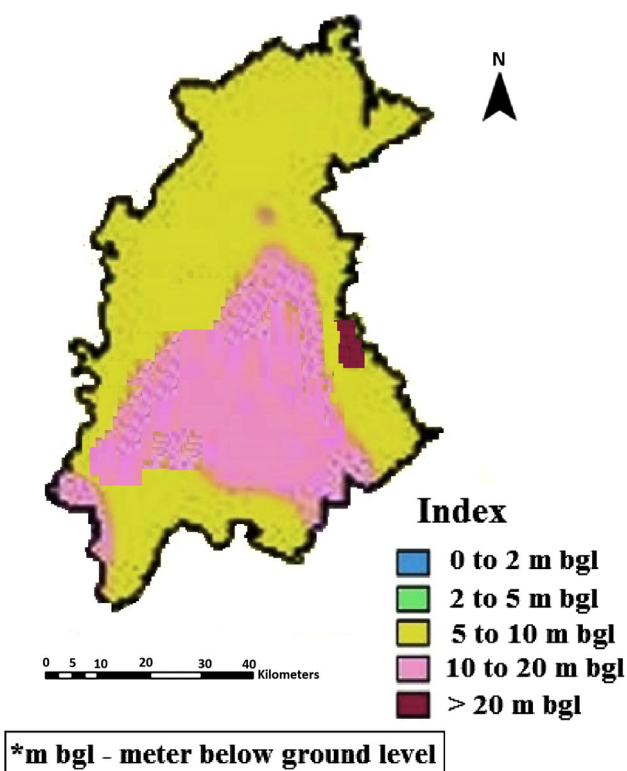


Fig. 5 Ground water level map of the study area

surrounding water resources (Reddy et al. 2010). The higher Cl^- concentration which is not in accordance with NO_3^- (encircled by broken lines) might be attributed to effect from higher evaporation rate during recharge process or exchange with rock minerals. For plot between NO_3^- and SO_4^{2-} (Fig. 6c), the points showing significant association indicate the origin from common source like the input from use of excessive amount of fertilizers (Zalidis et al. 2002). It is considered that SO_4^{2-} is one of the common ingredients of chemical fertilizers applied along with nitrogen compounds. Finally, it is observed that for saturated aquifer, the concentration of NO_3^- at any point/place is determined from NO_3^- content of the water recharging from the unsaturated zone above as well as from surrounding. Vertical movement of NO_3^- plume in case of saturated zone of the aquifer occurs slowly but distinct along the recharging flow line (Datta et al. 1997). Also improper drainage system causes enrichment of fecal matter with micro-organisms like *E. coli*, *Staphylococcus aureus*, *Proteus vulgaris*, *Salmonella typhi*, and *Pseudomonas aeruginosa* results into higher concentration of nitrate in the groundwater (Kumar et al. 2010). Finally, a part of soil with high drainage capacity or permeability and low forest to agricultural land, industrial and urban land use, leaching of nitrate from landfill or dump yard sites, and industrial effluents cannot be neglected for higher

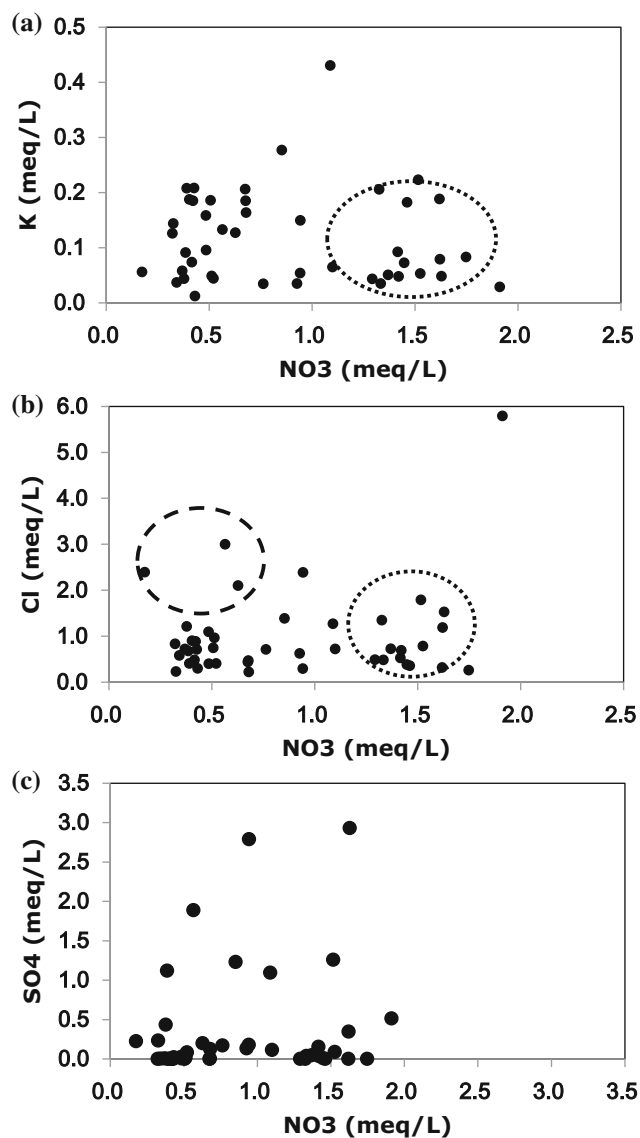
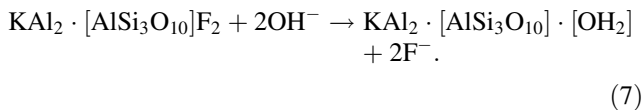


Fig. 6 Scatter plot between NO_3^- versus a K^+ , b Cl^- , and c SO_4^{2-}

concentration of nitrate in groundwater samples. On the other hand, lower nitrate content at some location which has similar hydrogeological setup and land use could be due to denitrification and solute transport hindrance.

Fluoride concentration in the groundwater ranged from 0.31 to 2.87 mg/L with average 1.03 mg/L. Because the primary source of F^- is geogenic and its solubility in fresh water is low, F^- concentrations frequently are proportional to the degree of water-rock interaction. Outcropping bedrocks in the study area include granite, gneiss, sandstones, and shale, which comprised fluoride-bearing minerals like biotite, muscovite, K-feldspar, plagioclase, pegmatite, amphiboles, fluorite, and fluorapatite (Singh et al., 2013). At low pH, F^- remains adsorbed in clay due to its low solubility. The F^- solubility is lowest in the pH range of

5–6.5 (Adriano 1986). However, at high pH (generally >7.5), the hydroxyl (OH^-), group replaces the exchangeable fluoride from minerals like biotite/muscovite and results in its enrichment in the groundwater and the possible reaction is shown in Eq. (7):



Henceforth, higher fluoride levels in groundwater in the study area might be due to the increase in pH and HCO_3^- content, where alkalinity leads to leaching of fluoride with the above-mentioned mechanism. The study area belongs to semi-arid region, and a high rate of evaporation leads to precipitation of the fluoride-rich salts over the uppermost layers of the soil after which the infiltrating water leaches fluoride salts and recharges the groundwater beneath it. Both pegmatites and amphiboles from Vindhyan supergroup have high concentrations of fluoride which leads to the dissolution and its enrichment in the groundwater bodies.

Hydrochemical Facies

The classification of water samples into different groups based on hydrochemical facies allows us to determine geochemical processes operating at a regional scale (Stuyfzand 1999). Piper diagram is widely used to present hydrogeochemical data to recognize and differentiate various water facies (Kumar et al. 2012). Based on the analyzed geochemical facies (Fig. 7), water samples were classified into following nine groups along with their percentage of total number of samples observed: (i) Na- HCO_3 type (60 %), (ii) Ca- HCO_3 (12 %), (iii) Na-Cl (10 %), (iv) Ca- NO_3 (4 %), (v) Na- NO_3 (4 %), and (vi) rest 10 % of the total sample were collectively being characterized by four facies, viz. Ca-Cl, Mg-Cl, Ca- SO_4 , and Na- SO_4 . Water facies types in the groundwater suggest that sporadic deviation of water samples from primary geochemical facies, i.e., Na- HCO_3 or Ca- HCO_3 , was due to accumulative effects of anthropogenic activities and subsurface geochemical reactions at local level.

Origin of Groundwater Mineralization

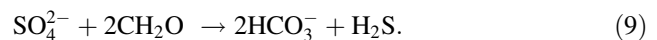
In order to understand the origin of groundwater mineralization in the study area, saturation index (SI) was calculated. Mineral saturation states with respect to solid phases of CO_2 (g), Anhydrite, Calcite, Dolomite, Fluorite, Hydroxyapatite, and Gypsum were computed as shown in Eq. (8), mentioned by Garrels and Christ (1965).

$$\text{SI} = \log_{10}(K_{\text{IAP}}/K_{\text{SP}}), \quad (8)$$

where SI is the saturation index, K_{IAP} is the ion activity product of particular solid phase, and K_{SP} is the solubility product of the phase. Based on the value of the SI, the saturation states were recognized as saturated (equilibrium; $\text{SI} = 0$), unsaturated (dissolution; $\text{SI} < 0$), and oversaturated (precipitation; $\text{SI} > 0$).

The calculated result of saturation index for different selected minerals in the water samples is shown in Fig. 8. The positive values of the calculated SI with respect to calcite, dolomite, and gypsum for majority of the water samples suggest their oversaturation with respect to this mineral which mainly has a geological origin derived from the abundant carbonate weathering in the plain area (Fig. 2).

Here, saturation with calcite along with undersaturation with respect to CO_2 (g) suggests the origin of Ca^{2+} and HCO_3^- in these samples, well described by Appelo and Postma (2005), and as shown in (Eqs. 4 and 5). However, focusing more on a higher concentration of bicarbonate in the water samples, another probable source was also deduced. From the scatter plot of bicarbonate versus sulfate (Fig. 9), the significant negative (inverse) correlation was found between them. It may be explained by the sulfate reduction phenomenon that is the result of the microbial decomposition of sulfate as shown in Eq. 9, and well described by Andersen (2001):



The wastewater with high organic matter (mainly from the agricultural and built-up regions as shown in central and northern part of the study area in Fig. 3) may be considered as the source of anaerobic sulfate reduction to produce bicarbonate and hydrogen sulfide with its characteristic odor.

The scatter plot between $\text{SI}_{\text{Gypsum}}$ and $\text{SI}_{\text{Anhydrite}}$ versus ($\text{Ca}^{2+} + \text{SO}_4^{2-}$) (Fig. 10) shows a significant positive correlation, suggesting that both calcium and sulfate are derived from the same origin, i.e., dissolution of gypsum and anhydrite, frequently found in the quaternary formations.

Isotopic Data and Salinity Origins

US Salinity Diagram

Groundwater usability for irrigation purposes can be judged by a mineral constituent of water and their effect on both plant and soil. EC and Na^+ play a vital role in determining the suitability of water for irrigation. Type and amount of the salts cause change in soil structure like porosity and permeability that indirectly affect the plant growth (Todd 1980; Domenico and Schwartz 1990). To

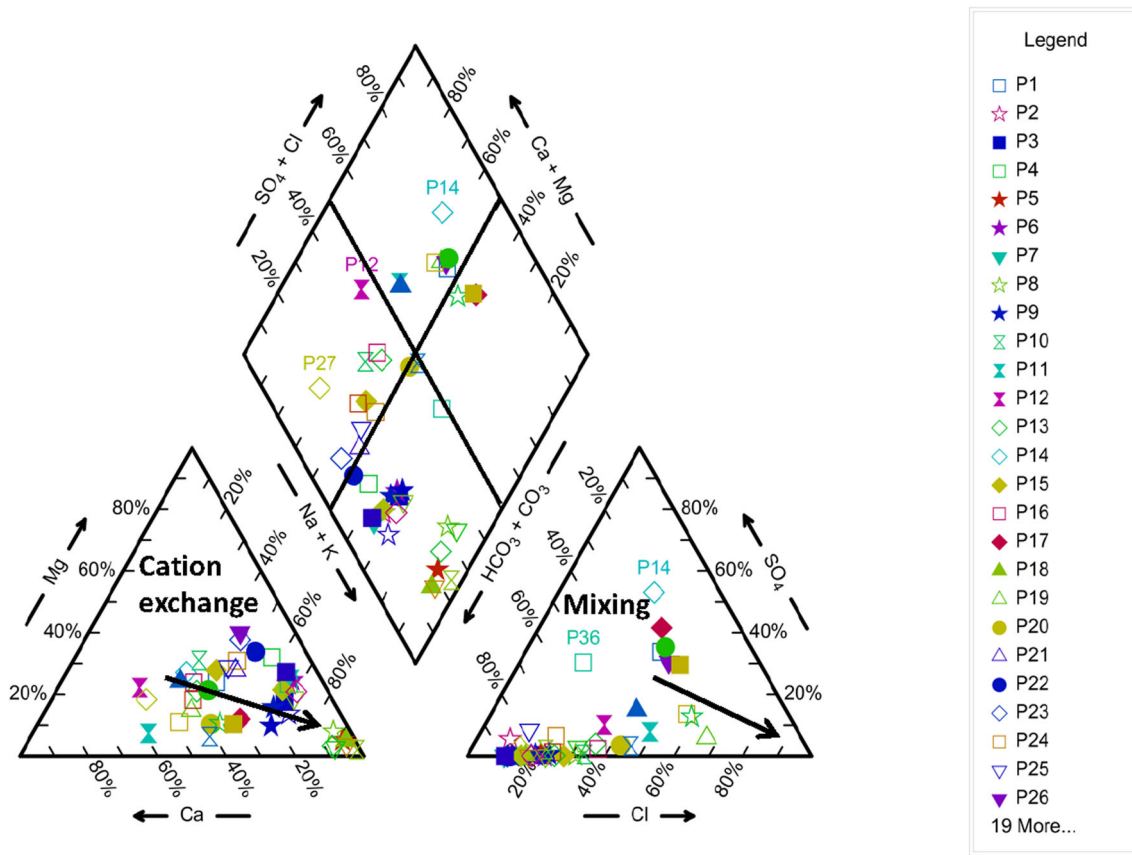
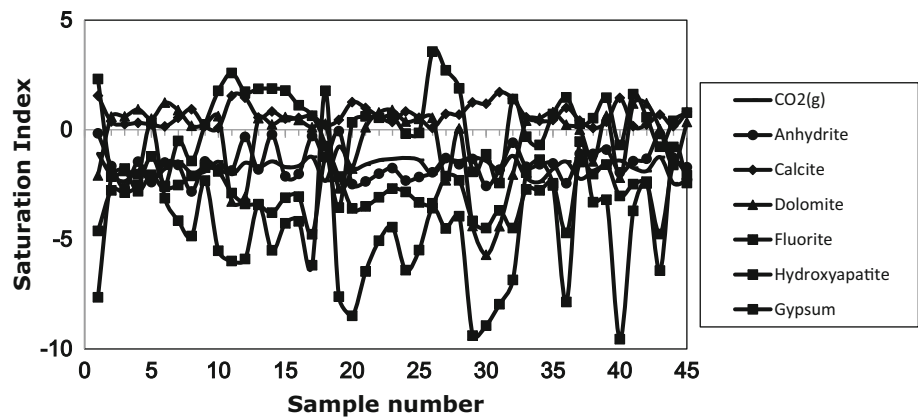


Fig. 7 Piper diagram showing water type in the study area

Fig. 8 Result of saturation index for selected minerals in water sample



determine the suitability of groundwater for agricultural purposes, indices such as sodium percentage (Na %), sodium absorption ratio (SAR), and residual sodium carbonate are important parameters. The sodium content, which is represented as sodium or soluble sodium percentage (Na %), can be calculated using Eq. 10, where all the concentrations are expressed in meq/L:

$$Na^+(\%) = \frac{Na^+}{(Ca^{2+} + Mg^{2+} + Na^+ + K^+)} \times 100. \tag{10}$$

Excess Na^+ combines with carbonate and leads to formation of alkaline soils. For the water samples, Na % value ranges from 21.5 to 95.6 % with average value of 53.7 %. Generally, % Na^+ should not exceed 60 % in irrigation waters; however, in the present study, it was found that 33 % (15 out of 45 in numbers) of the water sample is exceeding the recommended limit. Another criterion to judge suitability of water for irrigational use through plotting EC and SAR values of groundwater in the US salinity diagram is proposed by US Salinity Laboratory

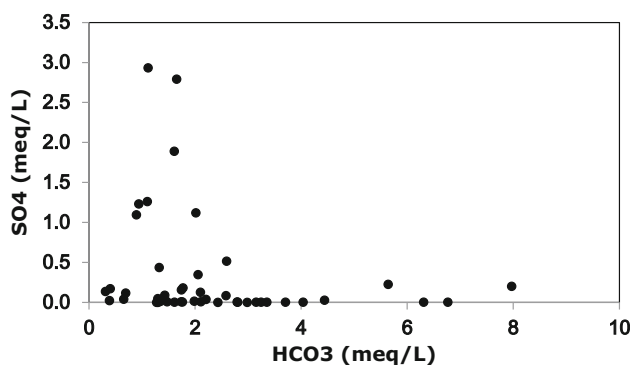


Fig. 9 Scatter plot between HCO_3^- and SO_4^{2-}

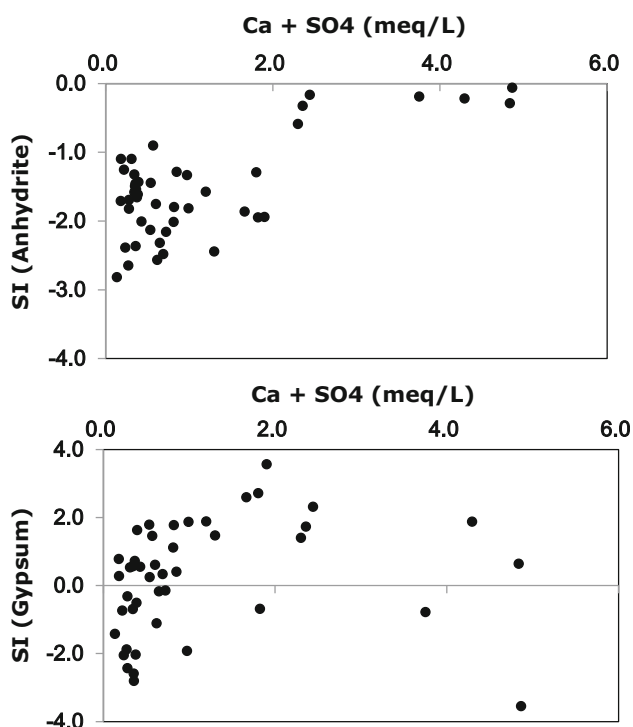


Fig. 10 Scatter plot between $\text{SI}_{\text{Gypsum}}$ and $\text{SI}_{\text{Anhydrite}}$ versus $(\text{Ca}^{2+} + \text{SO}_4^{2-})$

Staff (1954). SAR (sodium adsorption ratio) is defined as excessive sodium content relative to the calcium and magnesium which reduces the soil permeability and ultimately impedes the supply of water required for the crops.

The EC and SAR values of groundwater in the study area are shown in Fig. 11. It was found that most of the water samples fall in the category of C1S1 and C2S1, i.e., low salinity and sodium hazard and medium salinity and low sodium hazard category. All the water samples in these categories are considered to be of good quality for the agricultural purpose. Very few samples fall in the hazardous category, i.e., from medium to high salinity hazard and medium sodium hazard but may be considered acceptable for agricultural purposes (Table 2).

The evolution of groundwater quality can be traced out through trajectory lines for mixing of different groundwater bodies. It was found that water samples falling in the C2S2 and C3S2 category showed migration from fresh water system to saline water system. Processes like infiltration of sewage effluents from the rural households, leaching of surficial salt and untreated industrial waste, mixing of groundwater from different aquifers with variable Cl^- concentrations, and presence of secondary salinity, as indicated by high Cl^- and SO_4^{2-} , may cause the salinity difference between different water samples at spatial scale (Hasan et al. 2007). Sea water intrusion or fresh water-sea water mixing as a reason for salinization should be ruled out in this situation as the study area is located far from the coastal region but low precipitation followed by high evaporation may be the contributing factor in the region.

Stable Isotopic Chemistry

The relationship between $\delta^{18}\text{O}$ and δD values for groundwater samples is shown in Fig. 12. The value for $\delta^{18}\text{O}$ ranges from -9.64 to -7.37 ‰ with a median value of -8.54 ‰, whereas for δD , it ranges from -65.31 to -49.90 ‰ with a median value of -57.15 ‰. Most of the result points fall near the LMWL (drawn from the equation $\delta^2\text{H} = 8\delta^{18}\text{O} + 10$ (Craig 1961)) except fewer samples. Groundwater samples (Na- HCO_3 type) fell mainly along the local meteoric water line (LMWL), indicating that the origin of groundwater is meteoric and non-evaporated water is rapidly infiltrated into the saturated zone. However, the point away from the LMWL might be from non-equilibrium fractionation during evaporation and exchange with rock minerals. To support this hypothesis, the deuterium excess (d -excess) was calculated with equation (d -excess = $\delta^2\text{H} - 8\delta^{18}\text{O}$). It reflects the conditions that lead to kinetic isotope fractionation between water and vapor during primary evaporation in the oceans. It is a useful proxy to identify secondary processes that influence the atmospheric vapor content in the evaporation–condensation cycle in nature (Craig 1961). D -excess plotted versus $\delta^{18}\text{O}$ showed a negative correlation for the whole set of samples (Fig. 13). Here, decreasing trend in d -excess indicated the role of evaporation during the recharge processes for the change in water characteristics (Tsujimura et al. 2007). It is expected that, before reaching the saturated zone, irrigation water gets subjected to excessive evaporation in irrigated areas and later on acts as a salinization source. It was also inferred that groundwater salinization in intensively exploited agricultural fields was due to either evaporation during diffuse recharge or groundwater discharge via evaporation (Khan et al. 2008). Apart from evaporation,

Fig. 11 U.S. salinity diagram

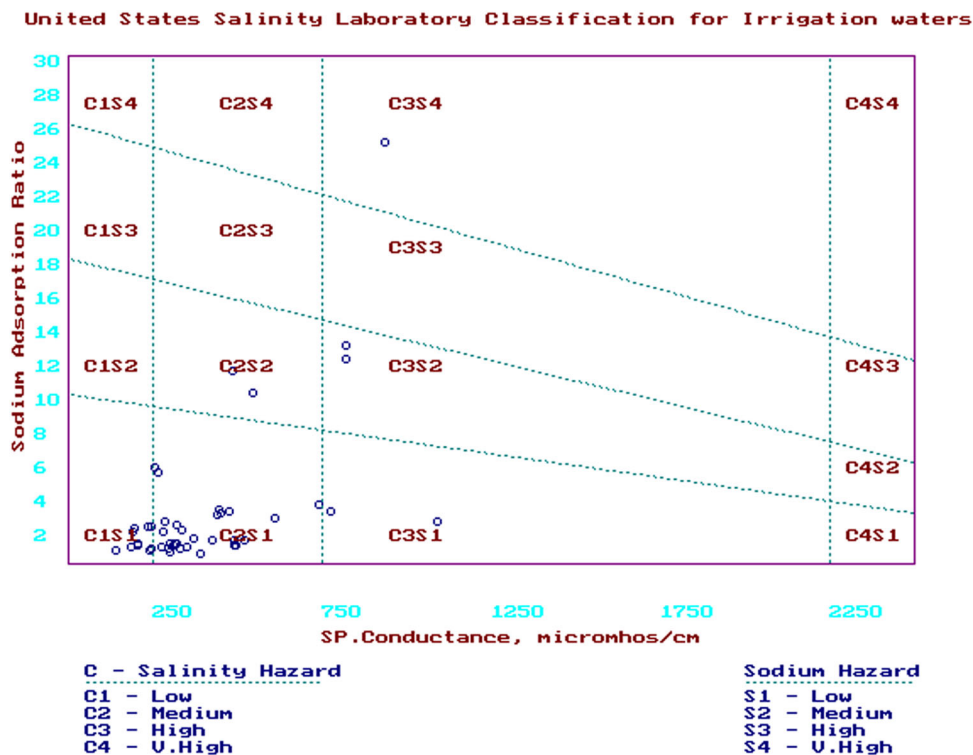


Table 2 Physicochemical characteristics of the water samples

Parameters	Average	Minimum	Maximum	SD
pH	—	7.16	8.02	0.20
EC (μS/cm)	411.38	140.50	1092.00	214.40
DO (mg/L)	2.68	0.77	7.56	1.77
Eh (mV)	190.88	100.30	457.00	85.87
HCO ₃ ⁻ (mg/L)	142.48	19.05	486.27	102.90
F ⁻ (mg/L)	1.31	0.10	4.87	1.08
Cl ⁻ (mg/L)	34.92	7.91	205.56	24.30
NO ₃ ⁻ (mg/L)	22.43	0.04	118.55	13.67
SO ₄ ²⁻ (mg/L)	16.34	1.23	140.69	10.24
PO ₄ ³⁻ (mg/L)	2.57	0.05	9.96	2.11
Ca ²⁺ (mg/L)	15.30	2.22	87.03	13.22
Mg ²⁺ (mg/L)	7.50	0.48	21.03	5.02
Na ⁺ (mg/L)	49.45	7.15	231.69	41.94
K ⁺ (mg/L)	4.54	0.47	16.77	3.26
Fe (mg/L)	12.18	0.30	43.60	13.25
Mn (mg/L)	0.71	0.01	4.33	0.93
NH ₄ ⁺ (mg/L)	0.42	0.02	1.12	0.34
H ₄ SiO ₄ (mg/L)	12.96	2.22	26.77	5.84
As(tot) (μg/L)	15.68	BDL	100.35	23.82
δ ¹⁸ O (‰)	-8.54	-9.64	-7.37	0.48
δ ² H (‰)	-57.15	-65.31	-49.89	3.09

BDL below detection limit

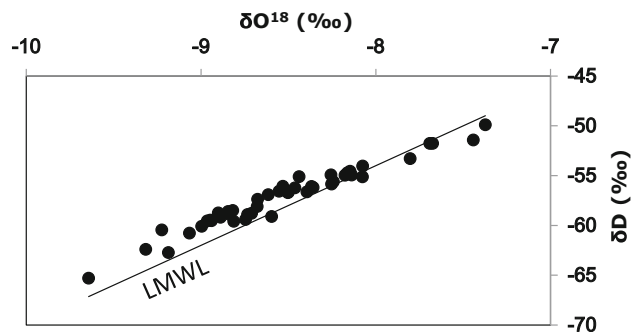


Fig. 12 Bivariate plot of δ¹⁸O and δD values for groundwater samples

exchange with rock minerals also contributed to change the water signature/type mainly Na–Cl type.

In order to make a clear distinction between different sources of salinity affecting groundwater in this study area, bivariate plot was made between δ¹⁸O and chloride of water samples (Fig. 14). Here basically three types of water samples were found. The first group of water samples having Cl⁻ concentration less than one meq/L and δ¹⁸O less than up to -8.0 ‰ was considered as water samples recharged with meteoric water (Diaw et al. 2012). The second group of water samples indicated water samples enriched in ¹⁸O with a small increase in chloride content

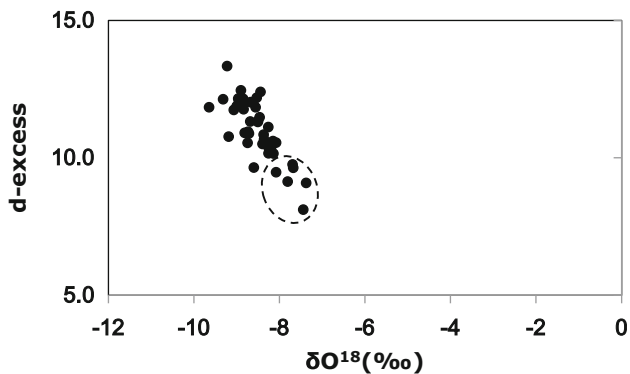


Fig. 13 Bivariate plot of $\delta^{18}\text{O}$ and d -excess values for groundwater samples

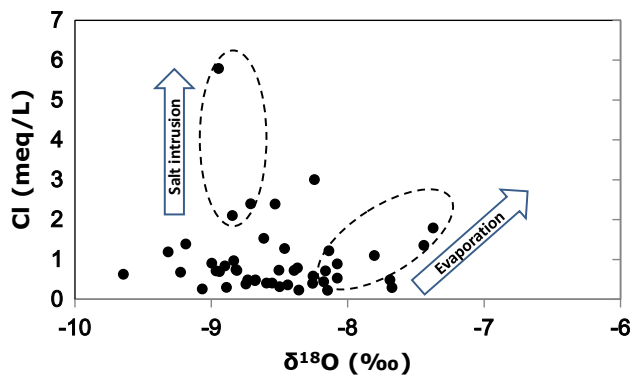


Fig. 14 Bivariate plot of $\delta^{18}\text{O}$ and Cl values for groundwater samples

because of evaporation. A third group of water samples indicated the approximate $\delta^{18}\text{O}$ values, which is equal as group 2 water samples but higher chloride content, could have been formed by salt intrusion. Since the study area is located far from the coast, chances of salt water intrusion may be ruled out. Another possibility for higher concentration of Cl^- might be related to the infiltration of sewage effluents from the rural households or mixing of groundwater from different aquifers with variable Cl^- concentrations.

Conclusion

The groundwater mineralization in the study area is not a homogenous process, but it is related to different sources and dynamics with spatial variation. The fresh shallow and deep groundwater chemistry is controlled by both natural conditions of rock–water interaction and anthropogenic effects. Result from isotopic trace elements clearly indicates that most of the water samples lie near LWML indicating their meteoric origin, whereas few water samples plotted away from the LMWL signifying exchange

with rock minerals and evaporation processes. Nitrate and fluoride enrichments are reported at the point scale, which needs further scientific attention. The alkaline nature of the groundwater triggers replacement of the exchangeable fluoride from minerals like biotite/muscovite and results in its enrichment. In addition, the granitic rocks which contain abundant fluoride-bearing minerals releases fluoride in the groundwater during the process of weathering. On the other hand, nitrate enrichment is mainly attributed to leaching from the untreated sewerage system and agricultural runoff containing nutrients from excess use of fertilizers.

Acknowledgments All authors would like to acknowledge the support from CIF facility of University of Tsukuba, Japan.

References

- Adriano DC (1986) Trace elements in the terrestrial environment. Springer, New York
- Agrawal D, Kumar P, Avtar R, Ramanathan AL (2011) Multivariate statistical approach to deduce hydrogeochemical processes in the groundwater environment of Begusarai district, Bihar. *Water Qual Expos Health* 3:119–126
- Andersen MS (2001) Geochemical processes at a seawater–freshwater interface. Ph.D. thesis. Technical University of Denmark. Lyngby, Denmark
- Anderson MP (1979) Using models to simulate the movement of contaminants through groundwater flow systems. *CRC Crit Rev Environ Control* 8:97–156
- Appelo CAJ, Postma D (2005) *Geochemistry, groundwater, and pollution*, 2nd edn. Balkema, Amsterdam
- Avtar R, Kumar P, Singh CK, Sahu N, Verma RL, Thakur JK, Mukherjee S (2013) Hydrogeochemical assessment of groundwater quality of Bundelkhand, India using statistical approach, water quality exposure and health. doi:10.1007/s12403-013-0094-2
- Basnyat P, Teeter L, Flynn K, Lockaby B (1999) Relationships between landscape characteristics and nonpoint source pollution inputs to coastal estuaries. *Environ Manag* 23(4):539–549
- Central Groundwater Board (CGWB) Ministry of Water Resources, Government of India (2010) *Groundwater quality in shallow aquifers of India*
- Craig H (1961) Isotopic variations in meteoric waters. *Science* 133:1702–1703
- Datta PS, Deb DL, Tyagi SK (1997) Assessment of groundwater contamination from fertilizers in the Delhi area based on O^{18} , NO_3 , and K^+ composition. *J Contam Hydrol* 27:249–262
- Diaw M, Faye S, Stichler W, Maloszewski P (2012) Isotopic and geochemical characteristics of groundwater in the Senegal River delta aquifer: implication of recharge and flow regime. *Environ Earth Sci* 66(4):1011–1020
- Domenico PA, Schwartz FW (1990) *Physical and chemical hydrogeology*. Wiley, New York
- Garrels RM, Christ CL (1965) *Solutions, minerals, and equilibria*. Harper and Row, New York
- Gupta SK, Deshpande RD (2004) Water for India in 2050: first-order assessment of available options. *Curr Sci* 86:1216–1224
- Hasan MA, Ahmed KM, Sracek O, Bhattacharya P, von Brömssen M, Broms S, Fogelström J, Mazumder ML, Jacks G (2007) Arsenic in shallow groundwater of Bangladesh: investigations from three different physiographic settings. *Hydrogeol J* 15:1507–1522

- Khan S, Rana T, Hanjra MA (2008) A cross-disciplinary framework for linking farms with regional groundwater and salinity management targets. *Agric Water Manag* 95:35–47
- Krishnan MS (1960) *Geology of India and Burma*, 2nd edn. Higginbothams Pvt. Ltd., Madras, pp 209–215
- Kumar P, Kumar M, Ramanathan AL, Tsujimura M (2010) Tracing the factors responsible for arsenic enrichment in groundwater of the middle Gangetic Plain, India: a source identification perspective. *Environ Geochem Health* 32:129–146
- Kumar P, Iwagami S, Yaping L, Mikita M, Tanaka T, Yamanaka T (2011) Multivariate approach for surface water quality mapping with special reference to nitrate enrichment in Sugadaira, Nagano Prefecture (Japan). *Environ Sys Decis* 31:358–363
- Kumar P, Tsujimura M, Nakano T, Minoru T (2012) The effect of tidal fluctuation on ground water quality in the coastal aquifer of Saijo plain, Ehime prefecture, Japan. *Desalination* 286:166–175
- Osborne LL, Wiley MJ (1988) Empirical relationship between land use-cover and stream water quality an agricultural watershed. *J Environ Manag* 26:9–27
- Ravindra K, Garg VK (2007) Hydro-chemical survey of groundwater of Hisar city and assessment of defluoridation methods used in India. *Environ Monit Assess* 132:33–43
- Reddy AGS (2012) Evaluation of hydrogeochemical characteristics of phreatic alluvial aquifers in southeastern coastal belt of Prakasam district, South India. *Environ Earth Sci*. doi:[10.1007/s12665-012-1752-6](https://doi.org/10.1007/s12665-012-1752-6)
- Reddy DV, Nagabhushanam P, Sukhija PS, Reddy AGS, Smedley PL (2010) Fluoride dynamics in the granitic aquifer of the Wailapally watershed, Nalgonda District, India. *Chem Geol* 269:278–289
- Reghunath R, Murthy TRS, Raghavan BR (2002) The utility of multivariate statistical techniques in hydrogeochemical studies: an example from Karnataka, India. *Water Res* 36:2437–2442
- Roth NE, Allan JD, Ericson DE (1996) Landscape influences on stream biotic integrity assessed at multiple spatial scales. *Landsc Ecol* 11(3):141–156
- Singh AK (2003) Water resources and their availability. In: souvenir, national symposium on emerging trends in agricultural physics, Indian Society of Agrophysics, New Delhi, 22–24 Apr, 2003, pp 18–29
- Singh V, Murthy RS, Pofali RM, Saxena RK (1983) Terrain analysis of Panna district, using Landsat imagery, *Jour. Ind Soc Photo-int Remote Sens* 11(1):43–48
- Singh KP, Malik A, Mohan D, Sinha S (2004) Multivariate statistical techniques for the evaluation of spatial and temporal variations in water quality of Gomti River (India)—a case study. *Water Res* 38:3980–3992
- Singh CK, Kumari R, Singh N, Mallick J, Mukherjee S (2013) Fluoride enrichment in aquifers of the Thar Desert: controlling factors and its geochemical modelling. *Hydrol Process* 27(17):2462–2474
- Srinivasamoorthy K, Chidambaram S, Prasanna MV, Vasanthavihar M, Peter J, Anandhan P (2008) Identification of major sources controlling groundwater chemistry from a hard rock terrain—a case study from Mettur taluk, Salem district, Tamil Nadu, India. *J Earth Sys Sci* 117(1):49–58
- U S Salinity Laboratory Staff (1954) *Diagnosis and improvement of saline and alkaline soils*. USDA Handbook 60. USDA: Washington
- Stuyfzand PJ (1999) Patterns in groundwater chemistry resulting from groundwater flow. *Hydrogeol J* 7(1):15–27
- Subramani T, Elango L, Damodarasamy SR (2005) Groundwater quality and its suitability for drinking and agricultural use in Chithar River Basin, Tamil Nadu, India. *Environ Geol* 47:1099–1110
- Todd DK (1980) *Groundwater hydrology*. Wiley, New York
- Tsujimura M, Abe Y, Tanaka T, Shimada J, Higuchi S, Yamanaka T, Davaa G, Oyunbaatar D (2007) Stable isotopic and geochemical characteristics of groundwater in Kherlen River basin, a semi-arid region in eastern Mongolia. *J Hydrol* 333(1):47–57
- Vijith H, Satheesh R (2007) Geographical Information System based assessment of spatiotemporal characteristics of groundwater quality of upland sub-watersheds of Meenachil River, parts of Western Ghats, Kottayam District, Kerala, India. *Environ Geol* 53:1–9
- World Health Organization (WHO) (2006) *Guidelines for Drinking-water Quality*. Third Edition. 1st Addendum to Vol. 1. WHO, Geneva. (http://www.who.int/water_sanitation_health/dwq/gdwq0506.pdf)
- Zalidis G, Stamatiadis S, Takavakoglou V, Eskridge K, Misopolinos N (2002) Impacts of agricultural practices on soil and water quality in the Mediterranean region and proposed assessment methodology. *Agric Ecosyst Environ* 88:137–146